Very Cold Neutron Source Based on Nanodiamond Reflector

Aleksenskii A.[1], Bleuel M.[2], Bosak A.[3], Dideikin A.[1], Dubois M.[4], Korobkina E.[5], Lychagin E.[6,7,8], Muzychka A.[6], Nekhaev G.[6], Nesvizhevsky N.[9], Nezvanov A.[6], Schweins R.[9], Strelkov A.[6], Turlybekuly K.[6], Vul' A.[1], and Zhernenkov K.[6,10]

[1] Ioffe Institute, St. Petersburg, Russia
[2] National Institute of Standards and Technology, Gaithersburg, USA
[3] European Synchrotron Radiation Facility, Grenoble, France
[4] SIGMA Clermont (ICCF), Université Clermont Auvergne, Aubière, France
[5] The University of North Carolina, Chapel Hill, USA
[6] Joint Institute for Nuclear Research, Dubna, Russia
[7] Lomonosov Moscow State University, Moscow, Russia
[8] Dubna State University, Dubna, Moscow reg., Russia
[9] Institut Max von Laue – Paul Langevin, Grenoble, France
[10] JCNS at Heinz Maier-Leibnitz Zentrum (MLZ), Forshungzentrum Julich GmbH, Garching, Germany

JINR Awards Competition for Young Scientists and Specialists
December 15, 2021
online

Very Cold Neutrons (VCNs)

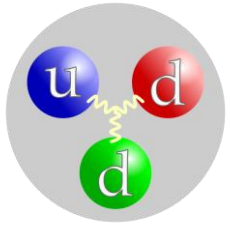

- Neutron mass = 1.675×10^{-27} kg;
- charge = 0;
- spin = ½;
- magnetic dipole moment = −1.913 μN.

Object & *Instrument* of research

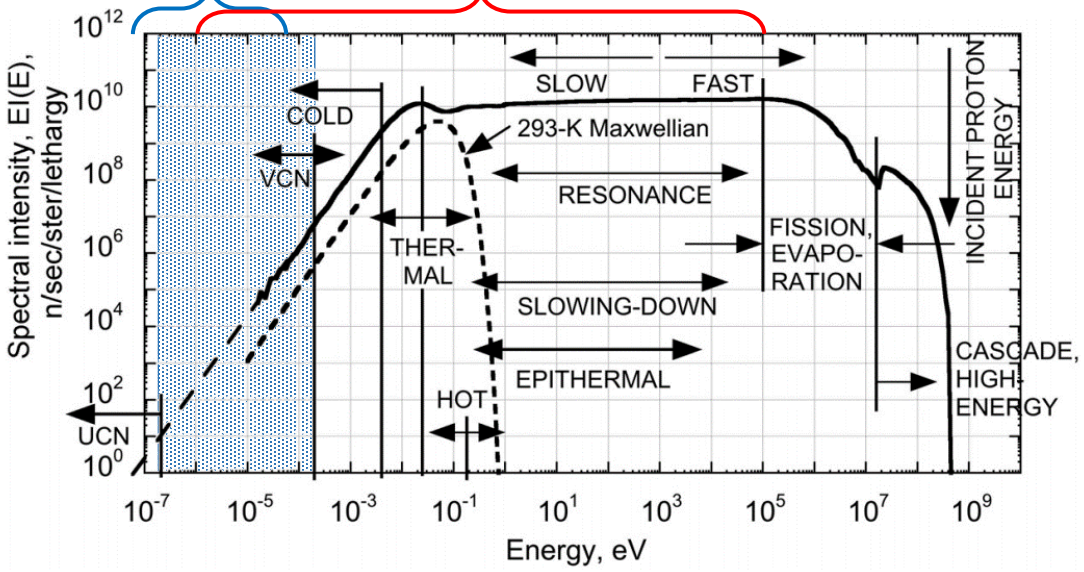

Fig. 1. The intensity spectrum for a spallation neutron source.

Typical VCNs:

- the energies are $E_{VCN} \approx$ 2–200 μeV;
- the wavelengths are $\lambda_{VCN} \approx$ 20–200 Å;
- the velocities are $v_{VCN} \approx$ 20–200 m/s.

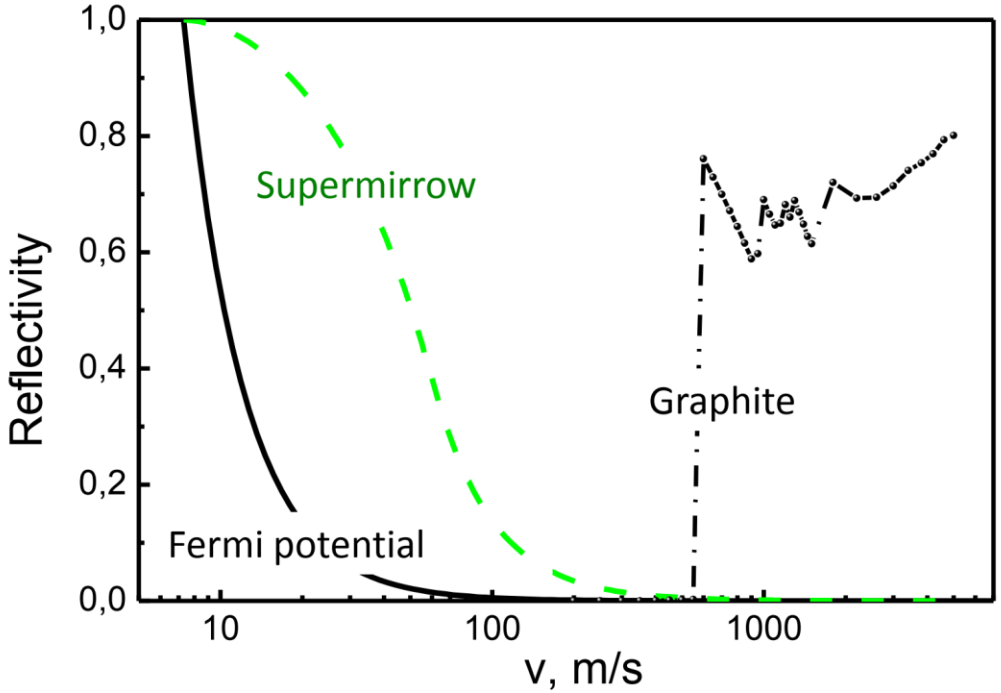

Fig. 2. The reflection probability (albedo) for isotropic neutron flux.

VCN Application

The VCN advantages are:

- long time of observation;
- large angles of reflections from mirrors;
- larger phase shift and as result more sensitive to contrast variation;
- large coherent length;
- large capture cross-section and big contrast at transmission;
- structure analysis of large molecular complexes; etc.

The main disadvantage is a low flux intensity!

Neutron techniques:

- SANS;
- spin-echo;
- TOF spectroscopy, in particular, high-resolution inelastic scattering;
- reflectometry, diffraction, microscopy, holography, tomography, etc.

Fundamental Physics:

- a search of extra-short-range interactions at neutron scattering;
- experiments with neutrons in a whispering gallery;
- beam experiment to measure of the neutron decay, etc.

VCN Reflector

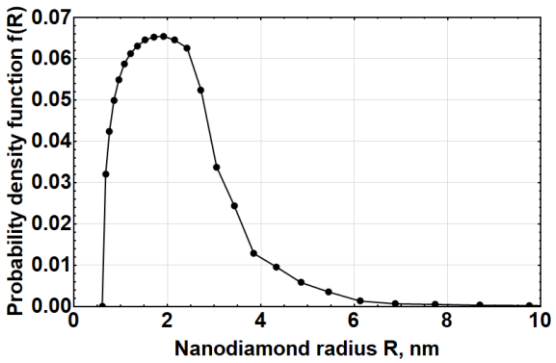

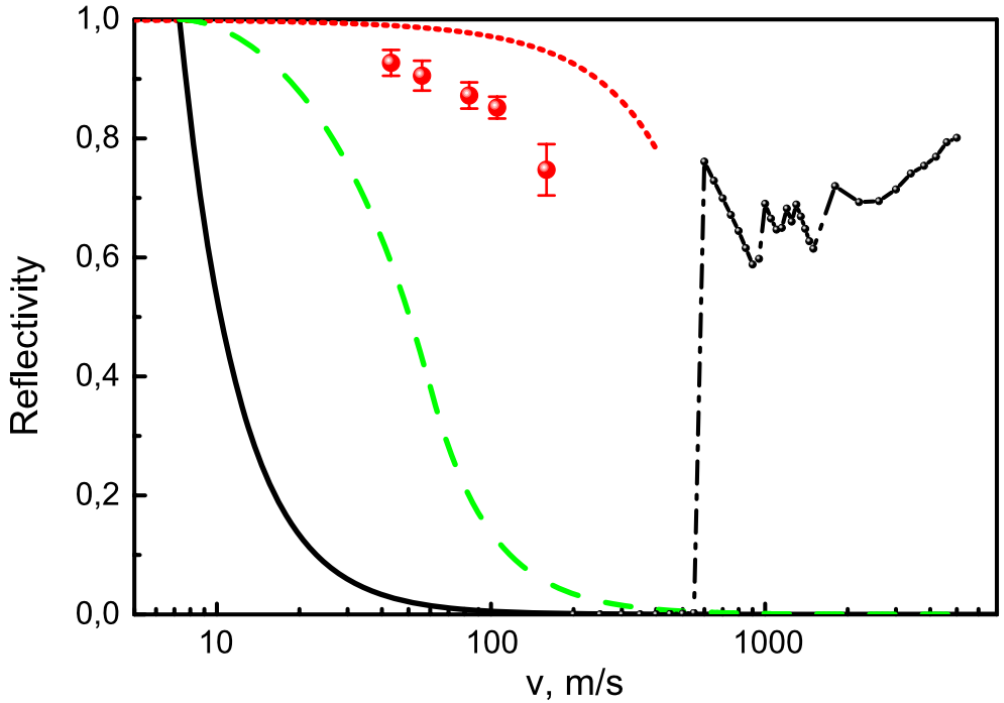

Criteria for the VCN reflector are
minimum losses and maximum reflection.

Detonation nanodiamonds (DNDs) are the ideal candidate!

$$P_{REF}^{max}: R_{opt} \approx 0.27\lambda$$

$$R_{opt}(\lambda) \approx 0.5 - 5.4\ nm,$$
$$\lambda_{VCN} \in [20, 200]\ \text{Å}$$

Positive Factors:

size distribution;

$b_{c.sc.}^{C} = 6.65\ fm;$

$\sigma_{c.sc.}^{C} = 5.55\ b;$

$\sigma_{abs}^{C} = 3.5\ mb;$

$\sigma_{in.sc.}^{C} \to 0\ (T \to 0);$

$\rho^{Diamond} \approx 3.5\ g/cm^3.$

Negative Factors:

~10 at. % of hydrogen,

$\sigma_{abs}^{H} = 0.33\ b;$

$\sigma_{in.sc.}^{H} = 108 \pm 2\ b;$

other impurities

< 0.15 at. %

neutron capture

neutron activation

Optimized Nanodiamonds

Implemented solutions:

the fluorination of DND

$C/H = 7.4 \pm 0.2$ (before)

$C/H = 430 \pm 30$ (after)

the additional purification of DND

$\Sigma_{abs}^{after} / \Sigma_{abs}^{before} \approx 0.58$

$\Sigma_{abs}^{H} \approx 0.2 \Sigma_{abs}^{after}$

But still significant activation!

the deagglomeration of DND

$P_{REF}^{after} / P_{REF}^{before} \approx 1.10$

$\rho_{bulk}^{after} / \rho_{bulk}^{before} \approx 3$

Preliminary results!

Today we have ~1 kg of the deagglomerated fluorinated DNDs (DF-DNDs). Is that a lot?

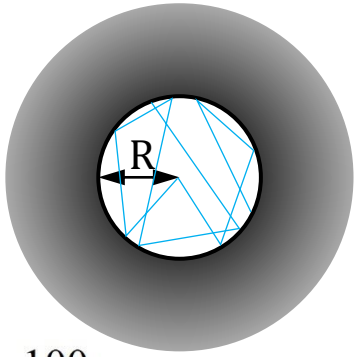

The incident neutrons are isotropic;
the powder thickness is infinite.
DF-DNDs density is equal to 0.56 g/cm^3.
DNDs density is equal to 0.19 g/cm^3.

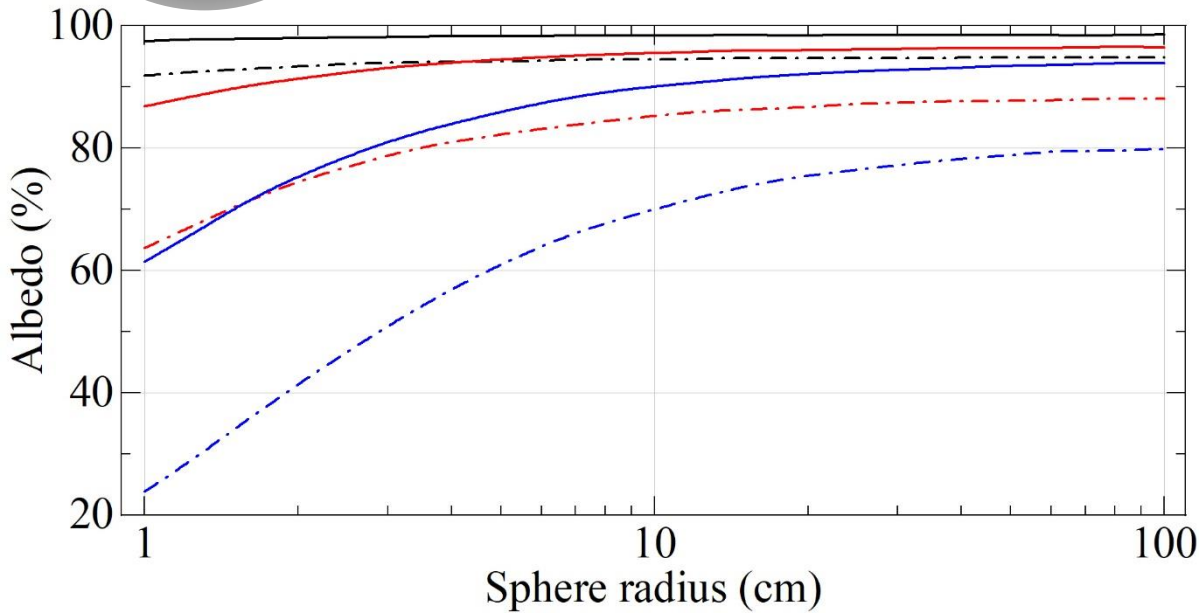

Fig. 3. Calculation of neutron albedo for the velocities of 50 m/s (black lines), 100 m/s (red lines), and 150 m/s (blue lines) for DF-DNDs (solid lines) and DNDs (dash-dotted lines) versus the cavity radius R.

Ideas of VCN Sources

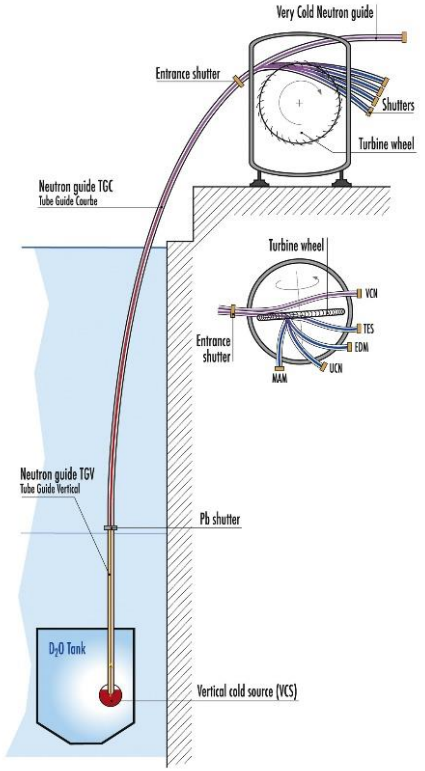

Fig. 4. The scheme of the PF2 beam ports at the ILL, Grenoble, including the PF2/VCN platform.

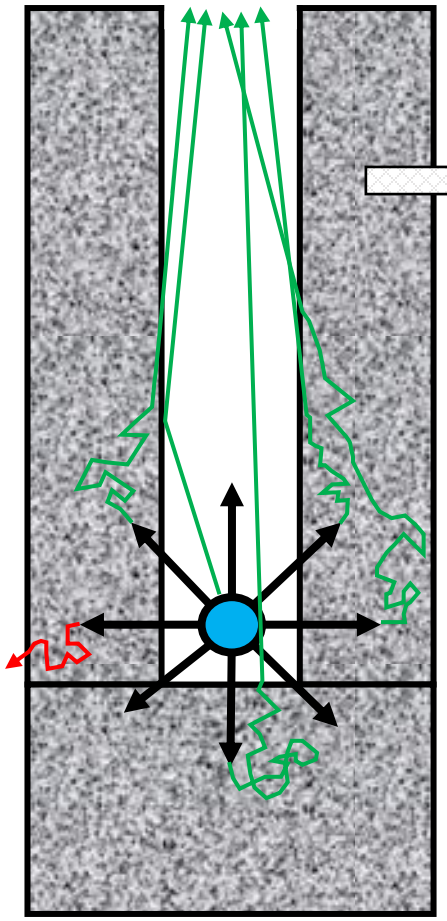

Fig. 5. The scheme of the possible VCN source.

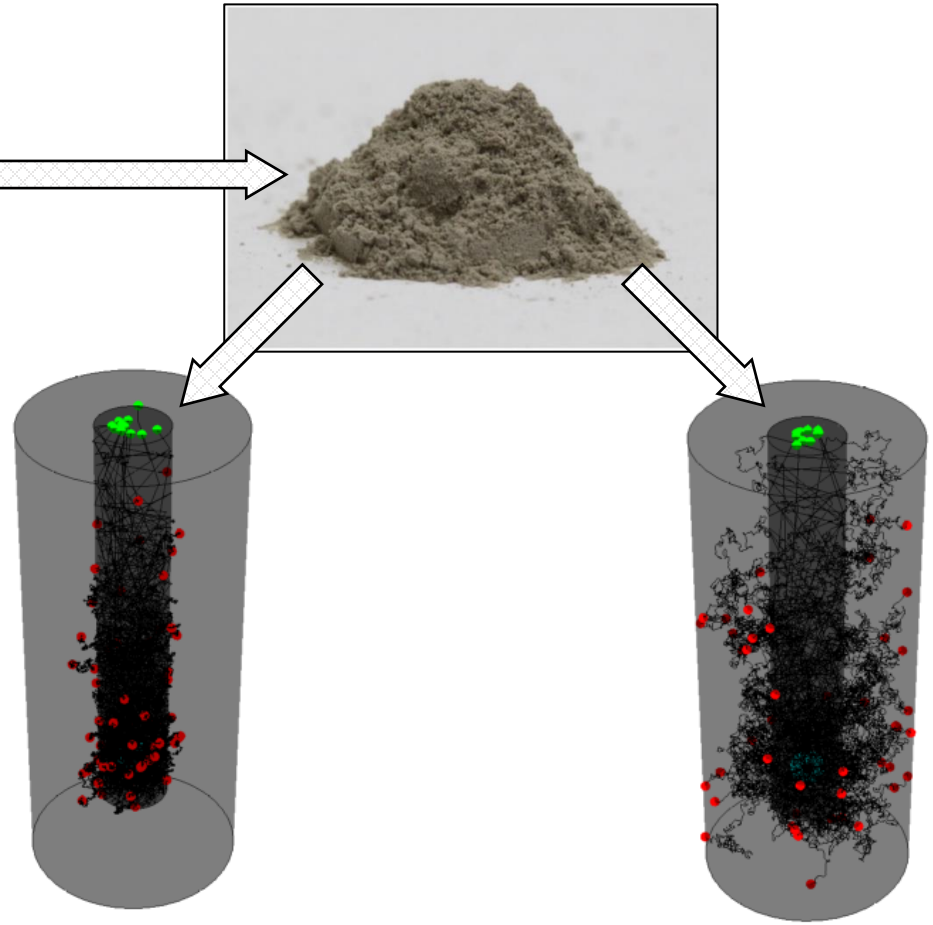

Fig. 6. First simulations for VCNs with velocities of 50 m/s (on the left) and 100 m/s (on the right) diffusing inside the tube made of fluorinated nanodiamond powder.

Directional Extraction of VCN

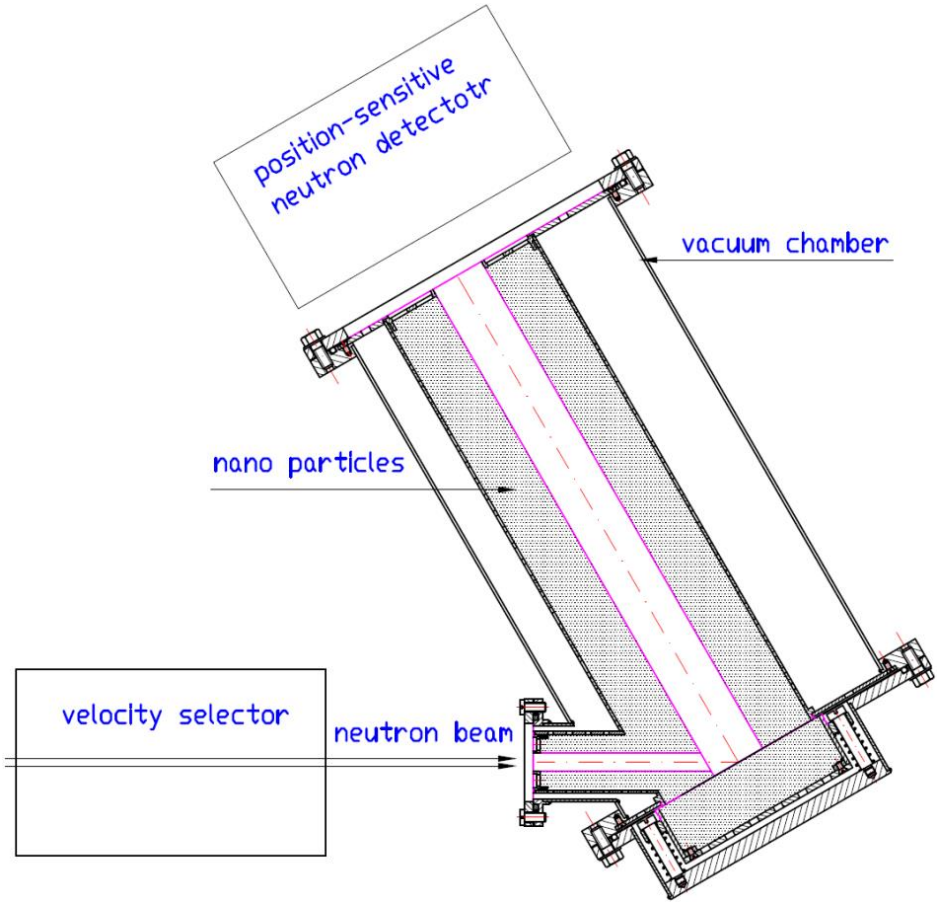

Fig. 7. The scheme of the experiment at the PF2/VCN, ILL, Grenoble (2017).

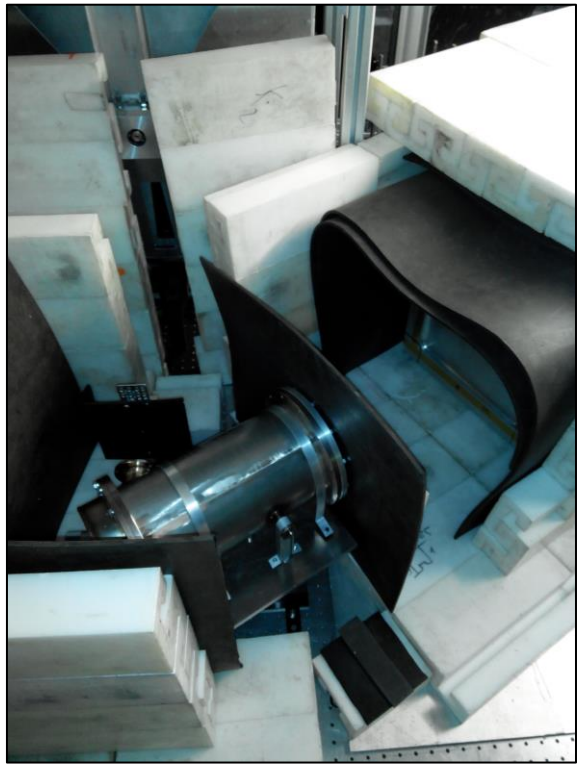

Preliminary experimental results: the total neutron flux extracted to the exit hole is increased up to 30 times related to flux without the reflector.
The gain factors of the directional extraction of VCNs are 11.3±0.4 for v = 57 m/s and 9.55±0.1 for v = 75 m/s.

The Prototype of a New VCN Source

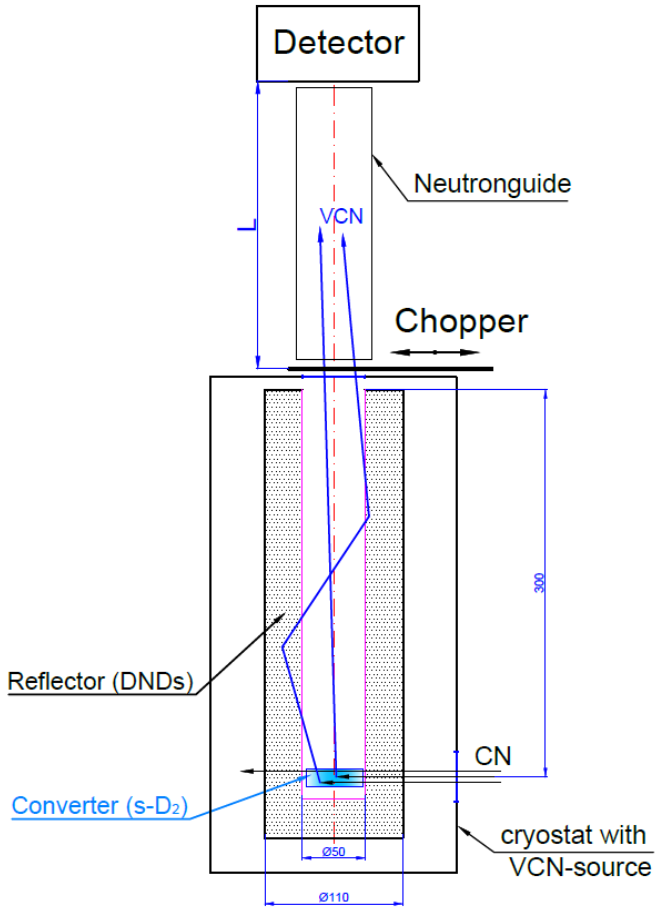

Fig. 8. The scheme of the upcoming demonstration of the VCN source prototype.

The converter tube is made from polytetrafluoroethylene (PTFE, Teflon™).

The inner diameter of the tube is 1 cm, the length is 5 cm, the wall thickness is 0.1 cm.

The temperature of solid ortho-deuterium is 5 K.

The reflector is fluorinated deagglomerated DNDs (FD-DND). Its bulk density is 0.87 g/cm^3 and the mean nanoparticle size is 3 nm. The inner diameter of the cylinder is ≈5 cm, the height is 20-30 cm, the wall thickness is 1-3 cm.

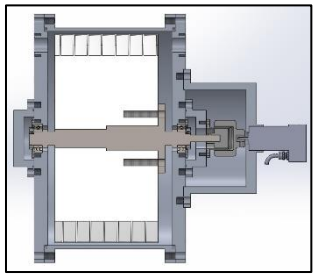

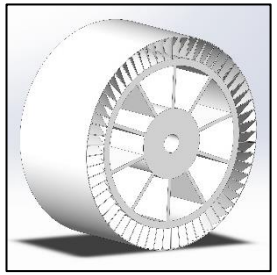

Fig. 9-10. The general scheme and the printed part of the optional velocity selector for VCN. It may be able to be used instead of the proposed chopper system.

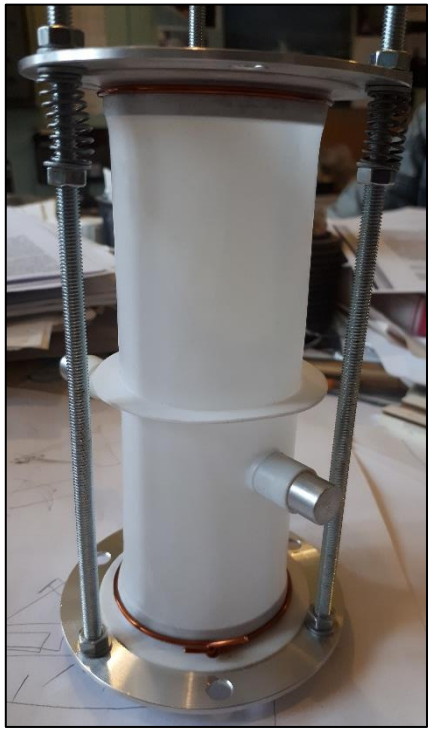

Fig. 11. The first example of the PTFE cylinder with the converter tube.

Estimating the VCN Source Productivity

Unfortunately, there is no data on the VCN production!

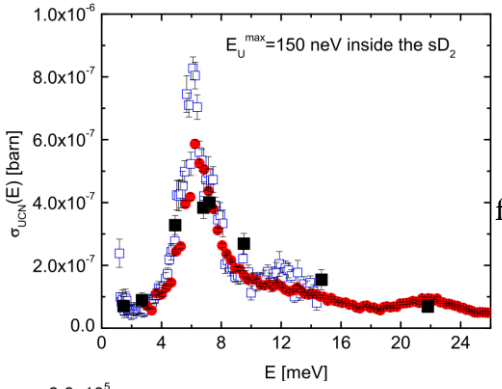

Fig. 12[1]. UCN production cross-section of c_o = 95.2% solid D_2. UCN energy range 0-150 neV inside the solid D_2. Cross-section determined by a integration of S(Q, E) along the free dispersion of the neutron (TS: "turbo-solid" - fast frozen solid deuterium (T =4 K)); data from IN4 measurements. Blue squares - E_0 =17.2 meV. Red filled circles - E_0 =67 meV. Black solid squares - data from measurements at the PSI.

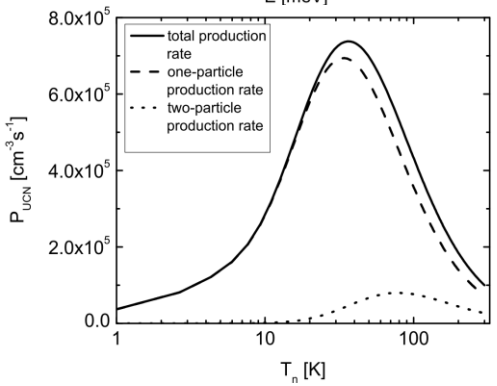

Fig. 13[1]. Calculated UCN production rate of c_o = 98% solid D_2 for different Maxwellian neutron spectra (effective neutron temperature T_n). UCN energy range - 0-150 neV inside the solid D_2. Neutron capture flux $\Phi_C = 1 \cdot 10^{14}$ cm^{-2} s^{-1}. Dashed line - one-particle production rate. Doted line - two-particle production rate. Solid line - total production rate.

VCN production cross-section approximation: $\sigma_{VCN} = \sigma_{UCN} \left(\frac{V_{VCN}}{V_{UCN}}\right)^3$, $V_{UCN} = 5.4\ m/s$ (150 neV); $[0, V_{VCN}]\ m/s$ – the VCN production range.

The converter volume is ≈ 4 cm^3.

Maxwellian spectrum of cold neutrons: $v_n^{mode} = 1000\ m/s$ ($T_n = 60\ K$).

Flux density is $J_0 = 10^{10}\ n/cm^2/s$.

VCN Production Rate

$[0,50]\ m/s$: $\Phi_{VCN}(50) = 1.6 \times 10^6\ n/s$;

$[0,100]\ m/s$: $\Phi_{VCN}(100) = 2.0 \times 10^6\ n/s$.

Attenuation Factors

"Useful" VCN limited by $v_n^{\rightarrow} = 6\ m/s$: $P_\Omega(50) \approx 4 \times 10^{-3}$; $P_\Omega(100) \approx 1 \times 10^{-3}$.

The duty cycle of the chopper disk: 10^{-2}

Expected Flux on the Detector

$$\boldsymbol{\Phi_{det}(50) = 8\ n/s;}$$
$$\boldsymbol{\Phi_{det}(100) = 16\ n/s.}$$

Estimating the Losses in the VCN Source with a Reflector

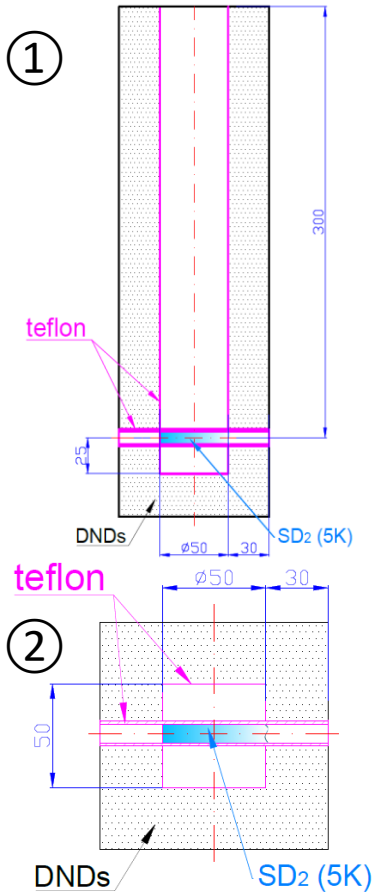

Fig. 14-15. Different source geometries for losses estimation.

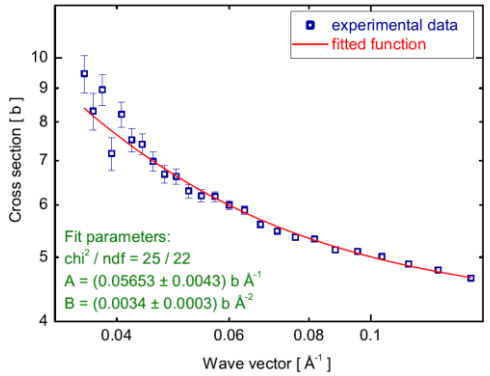

Fig. 16[2]. Total losses cross-section for the VCN in the s-D_2 (T = 5 K).

It is convenient to consider geometry ② for the losses estimation:
- the reflector's bottom is the main source of the "useful" VCN;
- if the albedo is ~90% the bottom volume will have almost isotropic VCN.

The cavity in such geometry ② will have the maximum flux.

Losses per flight through the cavity ($\approx \rightarrow =$)

$V_0 = 98\ cm^3$ - the cavity volume; $S_0 = 118\ cm^2$ - the cavity area.
$l_0 = 4V_0/S_0 = 3.3\ cm$ – the mean free path of a VCN in the cavity;
$V_D = 4\ cm^3$- the s-D_2 volume; $\rho_D = 0.2\ g/cm^3$ - the s-D_2 density;
$l_D = l_0 V_D/V_0 = 0.13\ cm$ – the VCN mean free path in the s-D_2.

The case of our source:

$$\sigma_{loss}^{D_2} = \frac{A}{k}$$

$$\sigma_{loss}^{D_2}(50) = \frac{0.0565}{0.078} = 0.72\ b;\ \sigma_{loss}^{D_2}(100) = \frac{0.0565}{0.156} = 0.36\ b;$$

$$\boldsymbol{P_{loss}^{D_2}(50) = 2.8 \times 10^{-3};\ P_{loss}^{D_2}(100) = 1.4 \times 10^{-3}.}$$

$V_w = 2.4\ cm^3$ - the PTFE volume in the walls;
$V_t = 1.7\ cm^3$ - the PTFE volume in the converter tube;
$V_{PTFE} = 2V_w + V_t = 6.5\ cm^3$ - the total PTFE volume;
$l_{PTFE} = l_0 V_{PTFE}/V_0 = 0.22\ cm$ - the VCN mean free path in the PTFE; $\rho_{PTFE} = 2.2\ g/cm^3$ - the PTFE density;
$\sigma_{loss}^{CF_2}(50) = 1.0\ b;\ \sigma_{loss}^{CF_2}(100) = 0.5\ b;$

$$\boldsymbol{P_{loss}^{PTFE}(50) = 6 \times 10^{-3};}$$
$$\boldsymbol{P_{loss}^{PTFE}(100) = 3 \times 10^{-3}.}$$

The converter tube creates two holes in the reflector. They can totally absorb neutrons in the worst-case.
$S_{hole} = 1.1\ cm^2$ - the hole area;

$$\boldsymbol{P_{loss}^{holes} = 2S_{hole}/S_0 = 1.9 \times 10^{-2}.}$$

Monte-Carlo simulation of the VCN reflection from the FD-DND in geometry #2 gives us:

$$\boldsymbol{P_{loss}^{FD-DND}(50) = 4 \times 10^{-2};}$$
$$\boldsymbol{P_{loss}^{FD-DND}(100) = 1.5 \times 10^{-1}.}$$

Estimating the Efficiency of the Reflector

The gain factor G of the VCN flux due to the usage of the proposed VCN reflector: $G \sim \frac{1}{P_{loss}}$

	$50\ m/s$	$100\ m/s$
$P_{loss}^{D_2}$	2.8×10^{-3}	1.4×10^{-3}
P_{loss}^{PTFE}	6.0×10^{-3}	3.0×10^{-3}
P_{loss}^{holes}	1.9×10^{-2}	1.9×10^{-2}
P_{loss}^{FD-DND}	4.0×10^{-2}	1.5×10^{-1}
Total losses P_{loss}^{min}	$\mathbf{\sim 6.8 \times 10^{-2}}$	$\mathbf{\sim 1.7 \times 10^{-1}}$

Table 1. List of all possible losses.

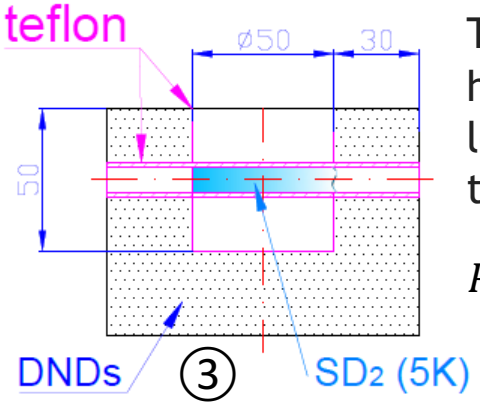

The geometry ③ has the maximum losses comparing to the others:

$$P_{loss}^{max} = P_{loss}^{min} + P_{loss}^{top},$$
$$P_{loss}^{top} = 1.6 \times 10^{-1}.$$

$$G_{max} \sim \frac{1}{P_{loss}^{min}}: \; G_{max}(50) \sim 15; \; G_{max}(100) \sim 6;$$
$$G_{min} \sim \frac{1}{P_{loss}^{max}}: \; G_{min}(50) \sim 4; \; G_{min}(100) \sim 3.$$

Accordingly, the expected neutron flux $\Phi'_{det}(V_{VCN})$ to the detector in the geometry ① with the reflector:

$$\Phi'_{det}(V_{VCN}) \in [\Phi_{det} \cdot G_{min}, \Phi_{det} \cdot G_{max}]$$

$$\boldsymbol{\Phi'_{det}(50) = 32 - 120\ n/s;}$$
$$\boldsymbol{\Phi'_{det}(100) = 48 - 96\ n/s.}$$

Close Future Plans

- The designing and developing of the vacuum and cooling systems.
- Finishing the study of the PTFE converter tube and the reflector walls.
- Testing the assembly at the FLNP JINR (IBR-2?), Dubna.
- Continue the development of the 3D-printed VCN monochromator.
- Monte-Carlo simulations:
  - new modified and purified DND powders;
  - different geometries of the reflectors / full-scale VCN sources;
  - models integration to the Geant4 code (thoughts about the Hovorun);
  - further model development for predicting the results of the final tests.
- The final tests of the prototype at the PF1B cold neutron beam at the ILL approximately in 2023.

Thank you all for your kind attention!

This research was funded by the JINR grant for young scientists №21-402-06, RFFI-18-29-19039, ERC INFRASUP P-2019-1/871072, and CREMLINplus (the grant agreement 871072).

The authors are grateful to V.A. Artem'ev for the fruitful discussions.

Alexander NEZVANOV, Ph.D.
nezvanov@jinr.ru
Frank Laboratory of Neutron Physics
Joint Institute for Nuclear Research, Dubna.